Optical Subnet Concepts for the Deep Space Network

K. Shaik and D. Wonica
Communications Systems Research Section

M. Wilhelm
Telecommunications Systems Section

This article describes potential enhancements to the Deep Space Network, based on a subnet of receiving stations that will utilize optical communications technology in the post-2010 era. Two optical subnet concepts are presented that provide full line-of-sight coverage of the ecliptic, 24 hours a day, with high weather availability. The technical characteristics of the optical station and the user terminal are presented, as well as the effects of cloud cover, transmittance through the atmosphere, and background noise during daytime or nighttime operation on the communications link. In addition, this article identifies candidate geographic sites for the two network concepts and includes a link design for a hypothetical Pluto mission in 2015.

I. Introduction

Communications systems are inherently capable of operating at higher antenna gain and modulation bandwidth as carrier frequency increases. Optical frequencies (approximately 10^{14} Hz) are several orders of magnitude higher than the operating carrier frequencies of the conventional RF communication systems (approximately 10^{10} Hz) in use today.

The promise of the large antenna gain and modulation bandwidth that become available at optical frequencies is the basic reason for the interest in the development of optical communication systems.

Optical systems also promise smaller size and mass and lower power consumption as compared to RF systems with similar performance characteristics. For planetary space missions, the advantage of reduced size, mass, and power requirements will allow more room for science instrumentation aboard a spacecraft.

The optical subnet concepts for the DSN reported in this article were developed, and their telemetry performance was estimated, for the Ground Based Advanced Technology Study (GBATS). The GBATS work was performed in conjunction with Deep Space Relay Satellite System (DSRSS) study contracts,[1,2] and its purpose was to initiate exploration of Earth-based alternatives to the

Raw or processed data are also stored in the archival subsystem for playback in case of GCF outage. The executive controller manages station activities automatically or manually through the command console, communicates with the outside world through the ground communications facility, and receives inputs from and sends commands to slave computers which include the pointing controller, the tracking controller, the figure controller, the signal processor, and the facility controller.

C. Ground Terminal Architecture

The system breakdown for the optical station is shown in Fig. 3. Note that subsystems other than the optical terminal are mentioned here for completeness and are not discussed any further. Additionally, the subsystems related to an optical uplink transmitter are not considered at this time.

1. Optical Terminal. An optical terminal consists of the following subsystems:

a. Telescope and Optics. The telescope subsystem provides an aperture to collect necessary photons for direct detection of incoming signals. The telescope employs a 10-m segmented primary mirror. There are 60 hexagonal segments, arranged in four rings, with each segment about 1.1 m in size (see Fig. 1). Other elements of the receiver telescope include a secondary-mirror assembly, a truss support structure, appropriate baffles to avoid the Sun, and other optics as needed. Each of the mirror assemblies includes mounts and the necessary actuators and baffles.

Table 1 provides a representative prescription for a Ritchey–Chretien Cassegrain telescope. The focal ratio for the 10-m segmented and hyperbolic primary is 0.5. The secondary mirror is 4.5 m from the primary mirror and is 1 m in size. The Cassegrain focus, where the optical communication instrument will be placed, is 3.25 m behind the primary. The image size at the Cassegrain focus for the usable diametric FOV (2 mrad) is about 16 cm.

b. Receiver Subsystem. The receiver subsystem consists of the optical communications instrument (OCI), which includes the receive beam-control optics (the beam-reducer optics, steering mirror, spectral filter, etc.), the tracking detector, and the communication detector. Fine pointing and tracking of the spacecraft are achieved by the OCI. Once coarse pointing is established by the acquisition, pointing, and tracking (APT) assembly, the OCI uses the communication signal as a beacon to aid in the fine ac-

quisition, pointing, and tracking process. The communication detector begins telemetry reception and transfers it to the signal-processing subsystem once tracking has been established.

Figure 4 shows a conceptual drawing of the OCI with its optics, spatial and spectral filters, steering mirror, and detectors. The received beam at the Cassegrain focus is corrected by a field corrector, spatially filtered by the field lens, and reduced and collimated by the reducer optics. The beam is spectrally filtered and steered by a two-axis steering mirror for fine pointing. A tracking detector is used to acquire, track, and center the received beam on the communications detector. The diametric FOV of the communications detector is restricted to 0.1 mrad.

c. Acquisition, Pointing, and Tracking. The APT assembly uses computer controlled azimuth–elevation gimbals. The telescope is mounted on the gimbals, and this mounting provides coarse pointing to and tracking of the user spacecraft. Initial coarse pointing coordinates, which will be used to bring the spacecraft within the telescope FOV, will be provided by the DSN. The network configurations studied here allow roughly 20 minutes to acquire the spacecraft and establish tracking.

Table 2 provides estimates of the pointing and tracking requirements. The coarse pointing requirement (0.2 mrad) is chosen to be an order of magnitude less than the useful Cassegrain FOV. The fine pointing requirement (0.01 mrad) is an order of magnitude less than the communication detector's FOV. The tracking rate is consistent with sidereal tracking requirements for deep space spacecraft. If the ability to track highly elliptical orbits (HEO's) is considered necessary, the tracking and slew rates must be revised upward as needed.

d. Environmental Housing. The environmental housing will consist of a protective dome over the telescope structure. Figure 5(a) shows a conceptual diagram for the dome when the dome is closed. It is similar to the dome built for the Air Force Starfire Optical Range's 3.5-m facility in New Mexico. The dome protects the telescope from catastrophic failure due to severe weather and protects optical coatings on the primary and the secondary from premature degradation. Figure 5(b) shows the telescope fully exposed under normal operating conditions when the dome is folded down to the pier.

D. Configuration of the User-Spacecraft Terminal

The user spacecraft terminal configuration used in this article is based on a TRW concept for a future optical

they use the same 10-m optical station and the same basic operations concept, each subnet offers unique advantages and disadvantages. Each subnet is designed to provide high weather availability. A detailed characterization of the two concepts and the reasons for selecting the number of stations in each case are provided in Section IV.

It is assumed that each station will require less than 20 minutes to acquire, track, and lock onto the incoming optical beam for both the LDOS and the COS concepts.

Figure 7(a) depicts network geometry for an LDOS showing three ground stations, and Fig. 7(b) depicts geometry for a COS network showing two of the clusters, each with three stations. Telemetry received by the available station for each subnet concept is demodulated and sent to the station data processing subsystem for one of three purposes: processing and formatting, storage in the archival subsystem, or for transmission in raw form to JPL's NOCC for distribution to end users. The stations are connected to the existing DSN infrastructure via the GCF.

IV. Performance Analysis

To develop optical network configurations that meet certain performance goals, several analyses were performed to identify a preferred approach. These efforts included the development of a propagation model, a weather model, an ideal-coverage model for the COS and the LDOS concepts, and availability assessments for various network configurations. For illustrative purposes, two network configurations, one from among the COS concepts and one from among the LDOS concepts, were selected for detailed study. For these two configurations, an LDOS with six stations and a COS with three clusters of three stations (COS 3 × 3), a coverage analysis was made for ideal conditions, as was a telemetry performance projection for a Pluto mission in the year 2015.

A. Propagation Model

Earth's atmosphere has a dominating impact on the propagation model for ground-based optical communications. Propagation loss and sky background radiance are two significant factors. Propagation loss, that is, loss due to transmission through the atmosphere, can be predicted using semiempirical models under various operating conditions. The problem of opaque cloud cover is studied in Section IV.B, where a weather model is produced.

The U.S. Standard Atmosphere 1976 model was used in this study to evaluate the effects of station altitude, meteorological range (i.e., visibility), and zenith angle. Section IV.A.1 shows that the impact of using atmospheric

models other than the U.S. Standard Atmosphere 1976 is very small.

It is also important to study the impact of sky background noise on optical communications, especially the impact during daytime operations. This is addressed in Section IV.A.5. The results are used to develop average telemetry rates for daytime operations in Section IV.F.

1. Atmospheric Transmittance Model. LOW-TRAN7, a transmittance model developed by the Air Force Geophysics Laboratory (AFGL) for visible and infrared wavelengths, was used to calculate propagation effects on wavelengths of interest, including 532 nm. The results of using the U.S. Standard Atmosphere 1976, mid-latitude winter, and mid-latitude summer atmospheric models on the transmittance, which was supplied by LOW-TRAN7, are shown in Fig. 8(a). The curves shown for all the models assume the presence of high cirrus clouds, a 2.3-km altitude for the ground station, a 17-km meteorological range (visibility), and a zenith path through the atmosphere. Since the atmospheric transmittance models do not differ significantly from each other, the U.S. Standard Atmosphere 1976 model was used to calculate nominal spectral transmittance under all operating conditions.

2. Spectral Transmittance Versus Altitude. Figure 8(b) shows the transmittance for selected altitudes as predicted by LOWTRAN7. In the ideal-coverage model, the station altitude (2.3 km) of the Table Mountain Facility (TMF) was used as the baseline for the optical stations. Altitudes for the actual locations were used once specific LDOS and COS configurations were developed.

3. Spectral Transmittance Versus Meteorological Range. Varying meteorological range (visibility) will have an impact on the transmittance of the optical beam. Figure 8(c) shows the spectral transmittance for selected visibilities for wavelengths between 0.4 and 2.0 μm. A meteorological range of 17 km (defined as clear) was used as the basis for all calculations in this article.

4. Spectral Transmittance Versus Zenith Angle. The most dominant factor influencing the transmittance of the optical beam through the atmosphere is the operational zenith angle during telemetry reception. Figure 8(d) is a LOWTRAN7 plot of spectral transmittance for selected zenith angles for wavelengths between 0.4 and 2.0 μm. At a 70-deg zenith angle, the air mass through which the signal must propagate is about three times larger than the air mass at zenith. This is equivalent to about 17 dB of loss. In this article, the telemetry reception of the

Facility, the minimum propagation loss at $\zeta = 60$ deg is -4.7 dB. Choosing this as the acceptable propagation loss, $L_0 = -4.7$ dB, and with $q = 0.34$ at TMF, the availability of a single site for $L = L_0$ is found to be $\omega_1(L_0) = 0.66$. If there are three such independent and identical sites in a subnet within the LOS of the user spacecraft, then from Eq. (2), the subnet availability is found to be $\omega_3(L_0) = 0.96$.

2. Weather Availability. As previously mentioned, weather availability is a measure of station outage due to weather effects such as clouds, rain, and dense fog. Individual sites for an optical subnet were chosen for their good cloud-free statistics, and are located far enough apart, as determined by Eq. (1), to ensure independent weather from station to station. The availability of a single station is expected to be at least 66 percent. The availability of a given network configuration is discussed in Section IV.D.

C. Coverage Analysis

LOS coverage (or, more simply, coverage) is defined as the percent of time during a 24-hour period when an unobstructed path, excluding weather conditions, exists between one or more stations on Earth and the user spacecraft. The performance goal for all networks is to provide 100 percent coverage.

A ground-based network consists of Earth stations strategically placed around the globe to provide full coverage, 24 hours a day. Ideally, only two stations located near the equator and placed exactly 180 deg apart would be required to provide full coverage. However, the number of stations quickly increases due to the constraint of the minimum operational elevation angle of 15 or 30 deg, the fact that the stations cannot always be placed at the equator, and the need to have more than one station in the spacecraft LOS to provide high weather availability. Specific network configurations and the coverage they provide are presented in the following paragraphs.

D. Network Analysis

The most promising network concepts which provide high weather availability and full coverage of the ecliptic were introduced in Section III.B earlier. In this section, subnet concepts are described in greater detail under idealized conditions to provide a rationale for the selection of promising configurations. The selected configurations, an LDOS with six stations and a COS configuration with nine stations, were then studied under realistic conditions with reference to a Pluto mission in 2015. The coverage

curves and the telemetry rates are derived using actual site parameters, including longitude, latitude, altitude, and cloud-cover statistics, obtained from satellite data or in situ observations, and compared to the results obtained under ideal conditions.

1. LDOS Analysis. In this study, LDOS configurations were designed with six to eight ground stations spaced roughly equidistant from each other and placed around the globe near the equatorial region. An LDOS with five stations was not considered since the availability of this configuration is considerably below 90 percent (the percent required by the GBATS guidelines), and because the optical subnet would need to operate at very low elevation angles for a large fraction of the time.

Since the characteristic cloud systems calculated according to Eq. (1) are of the order of a few hundred kilometers in size, which is much smaller than the interstation distance, the adjacent stations will lie in different climatic regions and thus have uncorrelated cloud-cover statistics. Once specific sites were chosen, single as well as joint cloud-cover statistics for two or more consecutive sites were evaluated and used to predict link availability.

The probability of link outage for the LDOS configuration is low because (a) several stations are within the LOS of the user spacecraft, and (b) the stations lie in different climatic zones and hence their weather patterns are uncorrelated. Since the receiving sites are far apart, data with high spatial resolution on cloud-cover statistics are not needed. Existing data with a resolution of about 100 km are sufficient. However, further site surveys are needed to provide weather data with high temporal resolution. The weather data with high temporal resolution are needed to compute and predict short-term outage statistics accurately. Weather data with hourly or better temporal resolution will probably be needed to finalize site selection.

The distance between the receiving stations in the LDOS concept is very large; therefore, the full benefit of using optical wavelengths can be realized only when the user spacecraft points accurately to the designated receiving station in the subnet. Since the spacecraft can be 4–5 light hours from the Earth for some planetary missions, the weather availability of the subnet has to be predicted several hours in advance to designate the receiving station, and the location of the designated station must be uplinked to the user spacecraft terminal for pointing purposes.

a. LDOS With Six Ground Stations. The LDOS which consists of six optical stations located approximately 60 deg apart in longitude about the equatorial region is

spacecraft hands over the signal beam to the next cluster as the spacecraft rises sufficiently above the horizon. Since the intracluster distance between stations is of the order of a few hundred kilometers, cloud-cover data with much finer spatial resolution (a few tens of kilometers) than for the LDOS configuration are required. In addition, the requirements for obtaining site-specific cloud-cover data with sufficient temporal resolution, which were discussed previously, apply here as well.

An advantage of the COS concept over the LDOS is that there is no need to predict weather availability several hours in advance. All stations within a cluster monitor the user-spacecraft's transmitted beam jointly with little pointing loss. Additionally, there is no need to designate a receiving station and, therefore, no need to uplink such information to the user spacecraft.

a. COS With 3 × 3 Stations. The clustered optical subnet to be discussed in detail consists of nine stations located in three clusters of three stations (COS 3 × 3); the clusters are approximately 120 deg apart in longitude (approximately 14,000 km). This configuration provides 96 percent weather availability since the stations are located within a cluster at distances no more than a few hundred kilometers apart.

Ideal coverage curves to model a COS 3 × 3, with the clusters located 120 deg apart in longitude, are seen as a subset of the curves for the LDOS configuration with six stations, which is shown in Fig. 12. (Consider curves 1(a), 3, 5, and 1(b) only.) The assumptions about the sites are the same as those described for the LDOS with six stations (see above); however, it is assumed that only one site in the cluster is receiving telemetry. The weather availability of this configuration is 96 percent, and the telemetry line is at $\zeta = 60$-deg zenith angle, which is where the handing over to the following cluster takes place.

The geographical cluster locations chosen for the COS 3 × 3 are shown in Fig. 14. Table 5(a) provides a list of the specific geographical sites and their weather statistics. Like the sites chosen for the LDOS subnet, each COS 3 × 3 site has cloud-free days at least 66 percent of the time. In this configuration, each cluster is dedicated to a single user pass, resulting in a 96 percent probability that at least one optical station will have a clear LOS to the user.

Figure 15 shows the coverage curves for the COS 3 × 3 stations when data on one of the three actual geographical sites in each cluster are used for a Pluto mission in 2015. The actual sites used to obtain the coverage curves are TMF in California, Siding Spring Mt. in Australia, and

Calar Alto in Spain. The site-specific information used to obtain these curves includes altitude, longitude, and latitude, as well as Pluto's trajectory across the sky. Note that Pluto does not pass through the zenith for any of the sites.

Like the LDOS configuration discussed above, the characteristic performance of the optical channel at approximately 70 deg off zenith (hand-over) is the determining factor for telemetry performance. The telemetry curve for the Pluto mission is placed at −6.2 dB, compared to −4.7 dB for the ideal case. However, even with this change, two gaps exist in the LOS coverage, totaling about 4 hours per day. The LOS coverage provided by the COS 3 × 3 for a Pluto mission in 2015 is about 79 percent. As is the case with the LDOS concept, each optical terminal has about 20 minutes to acquire, track, and lock onto the incoming optical beam. The total network availability has not changed, since each cluster contains three sites in independent weather cells.

Although this configuration provides the same telemetry rate as the LDOS network with six stations and better weather availability, the gaps in coverage and the significantly larger number of stations required for the clustered concept are distinct disadvantages.

b. COS With 3 × 4 Stations. A total of 12 optical stations will be necessary in this subnet configuration (COS 3 × 4). The distance between clusters will be roughly 90 deg in longitude (approximately 10,000 km).

Table 5(b) shows a list of probable geographical sites for COS 3 × 4. Each cluster (numbered 1 to 4) contains three optical station sites to satisfy the ground rules for the COS concept discussed above.

3. Network Availability. Weather-related availabilities for the idealized network configurations are shown in the second column of Table 6. The probabilities have been calculated using the model described above, with $q = 0.34$ for each individual site. Additionally, the acceptable zenith angle loss, or the telemetry line, used to calculate availabilities for the ideal LDOS networks is consistent with a 60-deg zenith angle, and the link calculations shown in Sections IV.E and IV.F below are based on this assumption. The telemetry line, however, can be made consistent with a 75-deg zenith angle to increase network availability to 92, 95, and 96 percent for an LDOS with 6, 7, or 8 stations, respectively. The trade-offs to identify optimum position for the telemetry line were not performed.

For an actual LDOS with six stations for the Pluto mission, a telemetry line at a 70-deg zenith angle was used

Table 9 shows that a ground-based optical subnet can provide very high data rates. For the Pluto mission at 30 AU, the telemetry rate can be as high as 1716 kb/sec, about 8.5 dB higher than the baseline rate of 240 kb/sec. Daytime data rates are lower, as expected, but still provide improvement over the baseline performance.

The telemetry rate can be further improved by employing 12- to 15-m receiver apertures. The technology for photon buckets up to 15 m in size is within reach with low technical risk. Use of a larger aperture, for a given data rate, is expected to have a favorable impact on the user-spacecraft design. It will usually mean a user-spacecraft optical terminal with smaller mass, size, and power consumption.

V. Conclusion

Several alternative optical subnet configurations were considered in this article. It is seen that an LDOS with six stations can provide nearly full LOS coverage of the ecliptic and 81 percent weather availability. If higher availabilities

are needed, an LDOS with seven or eight stations can be used.

COS 3 × 3 under realistic conditions fails to provide full coverage (it provides approximately 79 percent). If the clustered concept for the optical subnet is desirable, a COS 3 × 4 with 12 ground stations will be required to provide full coverage, at least for the Pluto mission in 2015. The availability of both COS configurations is expected to be 96 percent. The COS configuration imposes an additional requirement over the LDOS configuration for locating appropriate specific sites. The clusters must be about 90 deg apart in longitude for COS 3 × 4, and intracluster station distances must be at least 150 km to ensure decorrelation of weather statistics. This may make it more difficult to find three specific sites within a given cluster when other requirements such as high altitude and reasonable accessibility are included.

A linearly dispersed optical subnet with six to eight stations is recommended, since it accomplishes the task with fewer ground stations than any other configuration considered here.

References

[1] K. Shaik, "Progress on ten-meter optical receiver telescope," *SPIE*, vol. 1635, edited by D. L. Begley and B. D. Seery, pp. 109–117, 1992.

[2] K. Shaik, "A Preliminary Weather Model for Optical Communications Through the Atmosphere," *The Telecommunications and Data Acquisition Progress Report 42-95, vol. July–September 1988*, pp. 212–218, November 15, 1988.

[3] K. Shaik and J. Churnside, "Laser Communication Through the Atmosphere," *Proceedings of the Twelfth NASA Propagation Experimenters Meeting (Napex XII)*, Syracuse, New York, pp. 126–131, June 9–10, 1988.

[4] J. Nelson, T. Mast, and S. Faber, "The Design of the Keck Observatory and Telescope," Keck Observatory Report No. 90, Keck Observatory, Mauna Kea, Hawaii, pp. 2–11, 1985.

[5] D. P. Wylie and W. P. Menzel, "Cloud cover statistics using VAS," *Nonlinear Optical Beam Manipulation, Beam Combining, and Atmospheric Propagation, Proceedings of the Meeting*, Los Angeles, California, January 11–14, 1988, pp. 253–259, 1988.

[6] *Greenhouse Effect Detection Experiment (GEDEX), 1992 Update*, CD-ROM, World Data Center for Rockets and Satellites, Code 902.2 DAAC, NASA Goddard Space Flight Center, Greenbelt, Maryland, 1992.

[7] The Association of Universities for Research in Astronomy (AURA), *The NOAO 8-m Telescopes* (now called Gemini 8-m telescopes), proposal to the National Science Foundation, AURA, Washington, DC, 1989.

Table 4(a). Linearly dispersed optical subnet with six ground optical stations.

Location	Altitude, km	Longitude, deg	Latitude, deg	Time zone	Cloud-free days/weather	Preexisting facilities and infrastructure
Southwest United States Table Mountain Facility, Calif.	2.3	118 W	34 N	−8	66%/arid[a]	Yes
Hawaii, United States Mauna Kea	4.2	155 W	20 N	−10	>69%/dry [7]	Yes
Australia Siding Spring Mountain	1.1	149 E	31 S	+10	67%/dry	Yes
Pakistan Ziarat	2.0	68 E	30 N	+5	69%/arid	Information NA
Spain/Northwest Africa Calar Alto, Spain	2.2	2 W	37 N	−1	67%/arid	Yes
South America Cerro Pachan, Chile	2.7	71 W	30 S	−4	77%/arid [7]	Yes

[a] ISCCP satellite data, obtained from [6].

Table 4(b). Linearly dispersed optical subnet with seven locations.

Location	Altitude, km	Longitude, deg	Latitude, deg	Time zone	Cloud-free days/weather	Preexisting facilities and infrastructure
Southwest United States Table Mountain Facility, Calif.	2.3	118 W	34 N	−8	66%/arid[a]	Yes
Hawaii, United States Mauna Kea	4.2	155 W	20 N	−10	>69%/dry [7]	Yes
Australia Siding Spring Mountain	1.1	149 E	31 S	+10	67%/dry	Yes
Nepal/South India	NA	NA	NA	+6	NA	Information NA
Saudi Arabia Jabal Ibrahim	2.6	41 E	21 N	+3	NA	Information NA
Spain/Northwest Africa Calar Alto, Spain	2.2	2 W	37 N	−1	67%/arid	Yes
South America Cerro Pachan, Chile	2.7	71 W	30 S	−4	77%/arid [7]	Yes

[a] ISCCP satellite data, obtained from [6].

Table 5(b). Clustered optical subnet locations. The network consists of three ground optical receiving stations in each of the four locations.

Location	Altitude, km	Longitude, deg	Latitude, deg	Time zone	Cloud-free days/weather	Preexisting facilities and infrastructure
Southwest United States						
Table Mountain Facility, Calif.	2.3	118 W	34 N	−8	66%/dry[a]	Yes
Mt. Lemmon, Arizona	2.1	111 W	31 N	−7	>60%/dry [7]	Yes
Sacramento Peak, New Mexico	3.0	106 W	35 N	−7	>60%/dry [7]	Yes
Australia						
Mt. Bruce	1.2	118 E	23 S	+8	NA	Information NA
Mt. Round	1.6	153 E	30 S	+10	NA	Information NA
Siding Spring Mountain	1.1	149 E	31 S	+10	67%/dry[a]	Yes
Pakistan						
Ziarat	2.0	68 E	30 N	+5	69%/arid	Information NA
Site not determined	—	—	—	—	—	—
Site not determined	—	—	—	—	—	—
Spain/Northwest Africa						
Arin Ayachi, Morocco	3.7	5 W	33 N	0	NA	Information NA
Tahat, Algeria	2.9	5 W	22 N	−1	NA	Information NA
Calar Alto, Spain	2.2	2 W	37 N	−1	67%/dry[a]	Yes

[a] ISCCP satellite data, obtained from [6].

Table 6. Network availability.

Network	Availability with ideal sites, percent	Availability with actual sites, percent
COS 3×3	96	96
COS 3×4	96	96
LDOS: six stations	88	81
LDOS: seven stations	91	—
LDOS: eight stations	94	—

Table 7. Network coverage.

Network	Coverage with ideal sites, percent	Coverage with actual sites, percent
COS 3×3	100	79
COS 3×4	100	—
LDOS: six stations	100	95
LDOS: seven stations	100	—
LDOS: eight stations	100	—

Table 8. Operational parameters for link calculations.

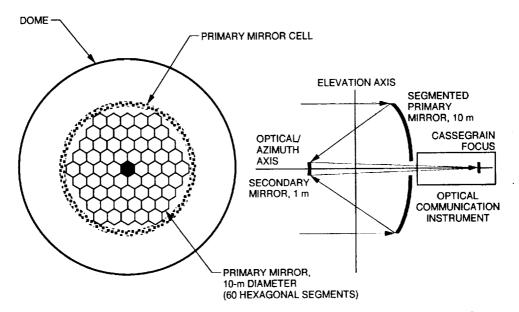| Parameter	Value
PPM alphabet size	256
Link distance, AU	30
Raw bit-error rate	0.013
Slot width, nsec	10

Fig. 1. Conceptual diagram of the 10-m telescope for the ground optical terminal (not drawn to scale). Primary diameter = 10 m; FOV at Cassegrain focus = 2.0 mrad; coarse pointing accuracy = 0.2 mrad; FOV at detector = 0.1 mrad; fine pointing accuracy = 0.01 mrad; and the blur diameter at focus $\leq$ 0.1 mrad.
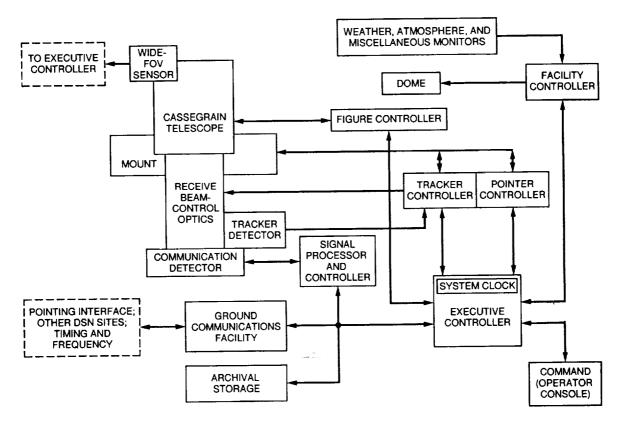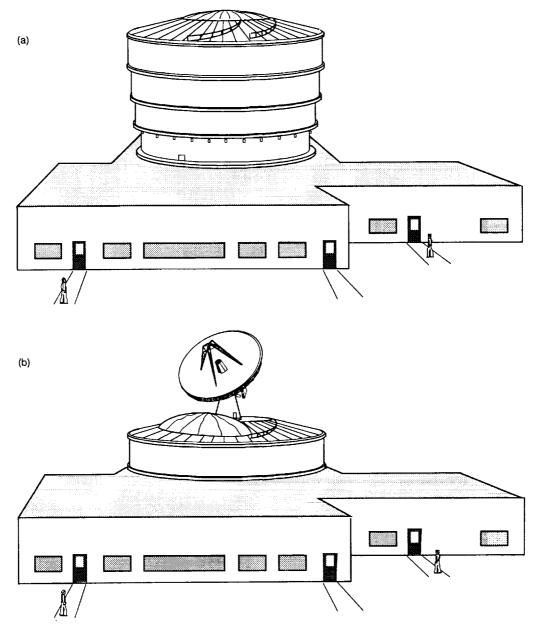

Fig. 2. Ground optical station block diagram.

(a)

(b)

Fig. 5. Typical protective dome for the receiver telescope: (a) closed and (b) open (not drawn to scale).
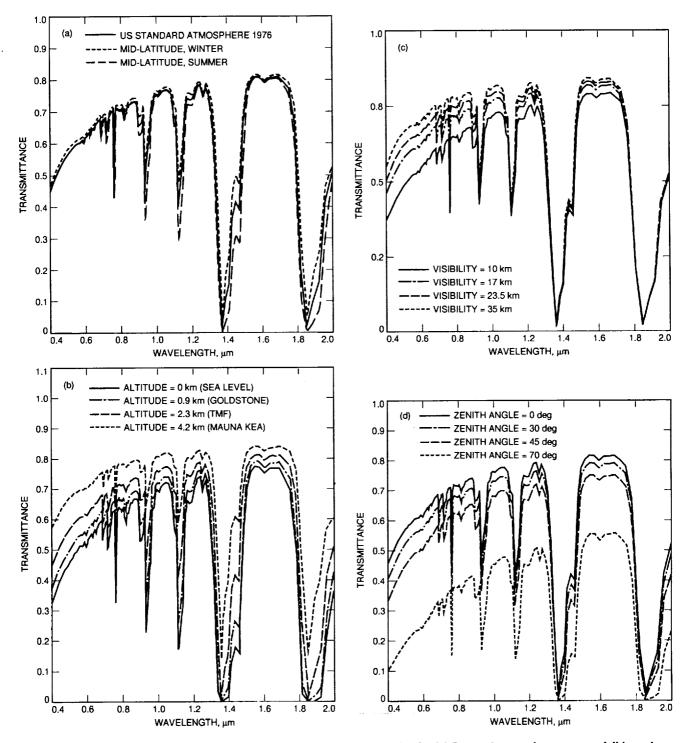
Fig. 8. Spectral transmittance data. All four diagrams assume high cirrus clouds. (a) Spectral transmittance over visible and near-infrared wavelengths for three LOWTRAN atmospheric models. (The diagram assumes a 2.3-km altitude, a 17-km meteorological range [clear], and a zenith path through the atmosphere). (b) Spectral transmittance for selected altitudes over visible and near-infrared wavelengths. (The diagram assumes the use of the U.S. Standard Atmosphere 1976 model, a 17-km meteorological range [clear], and a zenith path through the atmosphere). (c) Spectral transmittance for selected meteorological ranges (visibilities) over visible and near-infrared wavelengths. (The diagram assumes the U.S. Standard Atmosphere 1976 model, a 2.3-km altitude, and a zenith path through the atmosphere.) (d) Spectral transmittance for selected zenith angles over visible and near-infrared wavelengths. (The diagram assumes the U.S. Standard Atmosphere 1976 model, a 2.3-km altitude, a 17-km meteorological range [clear], and a slant path through the atmosphere).
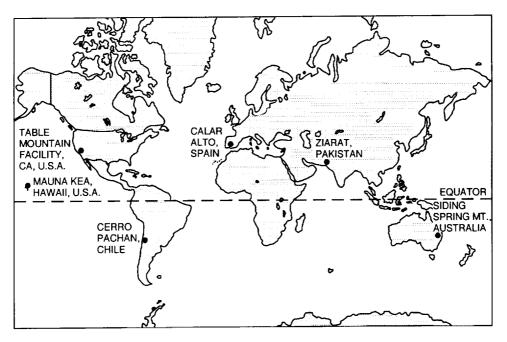
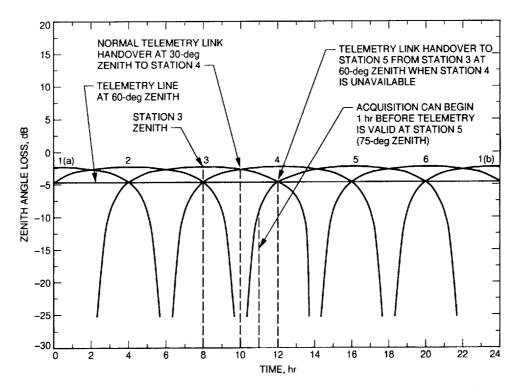Fig. 11. Geographical sites for an LDOS with six stations.

Fig. 12. Ideal-coverage curves over one day for an LDOS subnet with six stations 60 deg
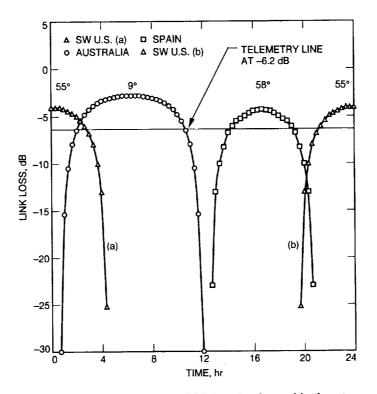apart in longitude in an equatorial belt.

Fig. 15. Coverage curves for a COS 3 × 3 subnet with nine stations for a Pluto mission in 2015. Zenith angles at local meridian for Pluto in 2015 are shown at the top of each curve. The sites used to calculate the coverage curves are TMF in California, Siding Spring Mt. in Australia, and Calar Alto in Spain (see Table 3). The coverage curve for the southwestern United States is shown in two halves: SW U.S. (a) and SW U.S. (b).

	Factor	dB
Laser output power (watts) Min Req'd peak power (watts) = .40E+04	7.00	38.5 dBm

Transmitter antenna gain
   Antenna dia. (meters)   =   0.750
   Obscuration dia.(meters)   =   0.000
   Beam width (microrad)   =   1.121
	0.160E+14	132.0

Transmitter optics efficiency	0.800	-1.0

Transmitter pointing efficiency
   Bias error (microrad)   =   0.100
   RMS jitter (microrad)   =   0.100
	0.893	-0.5

Space loss (30.00 AU)
Receiver antenna gain
   Antenna dia. (meters)   =   10.000
   Obscuration dia. (meters)   =   3.000
   Field of view (microrad.)   =   100.000
	0.890E-40
	0.446E+16
		-400.5
		156.5

Receiver optics efficiency	0.700	-1.5
Narrowband filter transmission Bandwidth (angstroms) = 0.010	0.600	-2.2
Detector Quantum efficiency	0.210	-6.8
Atmospheric transmission factor	0.240	-6.2
Received signal power (watts) Recv'd background power (watts) = 0.323E-17	0.228E-11	-86.4 dBm
Photons/joule	0.268E+19	154.3 dB/mJ
Detected signal PE/second	0.255E+07	64.1 dBHz
Symbol time (seconds)	0.290E-05	-55.4 dB/Hz
Detected signal PE/symbol	7.36	8.7
Required signal PE/symbol	3.69	5.7
Detected background PE/slot = 0.736E-04		
Margin	2.00	3.0

Table B-1. Additional sites of interest for an optical communications network.

Location	Altitude, km	Longitude, deg	Latitude, deg	Time zone	Cloud-free days/weather	Preexisting facilities and infrastructure
Roque de los Muchachos Observatory, Canary Islands, Spain	NA	16 W	29 N	−2	NA/dry	Yes
Fuente Nueva, La Palma Canary Islands, Spain	NA	16 W	29 N	−2	NA/dry	Yes
Jabal Toukal, Morocco	4.1	8 W	31 N	0	NA/dry	Information NA
Mulhecen, Spain	3.4	3 W	37 N	−1	67%/dry[a]	Information NA
Inaña, Tenerife, Canary Islands, Spain	NA	16 W	29 N	−2	NA/dry	Yes
Cerro Tololo, Chile	2.2	71 W	30 S	−4	77%/arid [7]	Yes
Llano del Hato, Venezuela	3.6	71 W	9 N	−4	NA/dry	Yes
Mt. Ziel, Australia	1.5	133 E	23 S	10	NA/dry	Information NA
Freeling Heights, Australia	1.1	139 E	30 S	10	NA/dry[b]	Information NA

[a] ISCCP satellite data, obtained from [6].

[b] A. Rogers, personal communication, Australian National University, Mount Stromolo and Siding Spring Observatories, Canberra, Australia, June 1993.